Influence of Sampling Interval and Number of Projections on the Quality of SR-XFMT Reconstruction

DENG Biao YU Xiao-Han[1)] XU Hong-Jie

(Shanghai Institute of Applied Physics, Chinese Academy of Sciences, Shanghai 201800, China)

Abstract Synchrotron Radiation based X-ray Fluorescent Microtomography (SR-XFMT) is a nondestructive technique for detecting elemental composition and distribution inside a specimen with high spatial resolution and sensitivity. In this paper, computer simulation of SR-XFMT experiment is performed. The influence of the sampling interval and the number of projections on the quality of SR-XFMT image reconstruction is analyzed. It is found that the sampling interval has greater effect on the quality of reconstruction than the number of projections.

Key words SR-XFMT, image reconstruction, sampling interval, number of projections

1 Introduction

Synchrotron Radiation based X-ray Fluorescent Microtomography (SR-XFMT) is a non-destructive technique by combining fluorescence microanalysis with tomographic techniques, which allows the reconstruction of a spatial distribution of non-radioactive elements inside a specimen from a set of fluorescence signals produced by monochromatic synchrotron radiation. It can map these elements simultaneously, in trace quantities, and at micron resolution. Since SR-XFMT was first proposed in 1986 by Boisseau[1], SR-XFMT has been modeled by several groups[2—7] and made as a powerful tool for several fields of research. The ability to determine elemental distributions within a sample has many real and potential applications, including the mapping of iodine distributions in thyroid tissue[8], the determination of element distributions in an individual fluid inclusion[9] and the reconstruction of distributions of heavy metals in roots[10], and so on[11—13].

In the SR-XFMT experiment, a monochromatic hard X-ray microbeam illuminates a thin line through a sample, stimulating emission of fluorescence X-rays from any element whose K-edge lies below the beam energy. By scanning and rotating the sample in the first-generation tomographic geometry, data are acquired allowing the reconstruction of the two- or three-dimensional distributions of the stimulated elements in the sample. In principle, it is possible to make a scan with a slice-to-slice separation equal to the transverse size of the beam, however, the full 3D scan of samples with several tens of microns dimensions is usually not feasible due to time constraints. For instance, the scan of a single slice of a sample of 300μm dimensions with 2μm spatial resolution and 1s/step dwell time takes already about 5h[14]. In order to reduce the time of data collection and increase the efficiency in the experiment, we have to increase the sampling interval or reduce the number of projections. But the quality of reconstruction will be influenced. It is important to select suitable sampling interval and the number of projections for reducing cost and improving the quality of reconstruction in SR-XFMT.

SR-XFMT will be an optional experimental tech-

Received 12 September 2006, Revised 1 November 2006

1) E-mail: yuxh@sinap.ac.cn

nique at SSRF (Shanghai Synchrotron Radiation Facility) hard X-ray micro-focusing beamline now under construction. In this paper, computer simulation of SR-XFMT experiment is performed. The influence of the sampling interval and the number of projections on the quality of SR-XFMT image reconstruction is analyzed. A conclusion on the relationship between the reconstruction quality and the sampling interval and the number of projections can be drawn. It is very useful for the real experiment study.

2 Principles of SR-XFMT

Figure 1 depicts a typical SR-XFMT experimental geometry. The coordinate system (x, y) is fixed in the laboratory system. The system (s, t) represents the rotating coordinate system associated with the specimen. To obtain a single SR-XFMT projection, the specimen is scanned through the monochromatic hard X-ray microbeam in translation along s. After each projection, it is rotated and the next projection is recorded. The procedure is repeated until a full rotation is completed in 180°. At each step the X-ray fluorescence excited by X-ray microbeam is recorded by the fluorescence detector. Two PIN diodes, one before and one after the specimen, are used for normalization and measurement of the transmission, respectively. The detection signal of a particular fluorescence line v of an atomic species i is given by

$$I_{iv}(s,\alpha) = C_{\rm det} I_0 \int_{-\infty}^{+\infty} \exp\left[-\int_{-\infty}^{t} \mu^{\rm I}(s,t')\mathrm{d}t'\right] \mathrm{d}(s,t) \times \exp\left[-\int_0^{\infty} \mu^{\rm F}(s,t)\mathrm{d}b\right] \mathrm{d}t = \int f(\alpha,s,t,\mu^{\rm I}) d(s,t) g_{iv}(\alpha,s,t,\mu^{\rm F})\mathrm{d}t \ , \qquad (1)$$

where I_0 is the initial intensity of the incident X-ray. $C_{\rm det}$ describes the detector efficiency and attenuation outside the sample.

$$f(\alpha,s,t,\mu^{\rm I}) = I_0 \exp\left[-\int_{-\infty}^{t'} \mu^{\rm I}(s,t')\mathrm{d}t'\right]$$

is the incident radiation intensity attenuated,

$$g_{iv}(\alpha,s,t,\mu^{\rm F}) = C_{\rm det} \times \exp\left[-\int_0^{\infty} \mu^{\rm F}(s,t)\mathrm{d}b\right]$$

is the fluorescence radiation intensity attenuated. $\mu^{\rm I}$ and $\mu^{\rm F}$ are the absorption coefficients at stimulating and fluorescent energy that can be calculated from absorption tomograms. $d(s,t)$ denotes the distribution of an element inside a specimen.

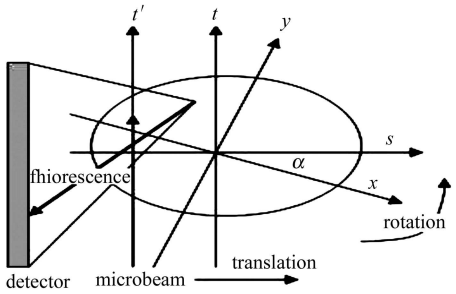

Fig. 1. Experimental geometry for SR-XFMT.

The goal of image reconstruction in SR-XFMT is to solve Eq. (1) for $d(s,t)$. Various approaches are available for the image reconstruction of the function $d(s,t)$: analytical reconstruction processes or the iterative reconstruction process. For instance Hogan[2] et al. have proposed an image reconstruction algorithm with attenuation-correction that involves correcting a straightforward FBP reconstruction of the measured projection data by dividing each pixel value by the average value of the attenuation experienced by this pixel. Others have proposed more intensive iterative approaches based on the use of singular-value decomposition (SVD)[3], algebraic reconstruction techniques (ART), and maximum likelihood expectation maximization (MLEM)[4]. All these approaches assume that all the needed attenuation maps (at both the incident and fluorescence energies) are known. Schroer[15] and Golosio[16] et al. have proposed more sophisticated iterative approaches that are applicable when only the incident beam attenuation map is known.

According to Hogan, the distribution of an element $d(s,t)$ can be approximated as:

$$d(s_0,t_0) \approx \frac{\tilde{I}_{\rm total}(s_0,t_0)}{\sum_{i=1}^{n} f_0(\alpha_i,s_i,t_i) g_0(\alpha_i,s_i,t_i)} \ , \qquad (2)$$

where the subscripts zero on f and g signify the appropriate absorption factors for the point (s_0,u_0); the tilde above $I_{\rm total}$ represents the operation of FBP. This algorithm has already been dealt with in theory

by Hogan et al. in simulation calculations, this leads to good results. In this paper, image reconstruction including attenuation effects correction from the simulation fluorescence data is achieved by the modified FBP.

3 Numerical simulation

In order to determine the influence of the sampling interval and the number of projections on the quality of reconstruction, we have conducted simulation studies of a numerical phantom using different sampling intervals and a number of projections. The computer simulations of SR-XFMT were performed on a biological specimen for distributing a metal element inside the specimen. Several assumptions were made in order to simplify the computation.

(1) We simulated data collection for a two-dimensional imaging geometry.

(2) The shape of the specimen used in the simulation was regular geometry.

(3) Attenuation was assumed to be uniform within the specimen. Fig. 2 depicts the object used as a simulated test sample. Its simulated chemical composition and distribution are reported in Table 1.

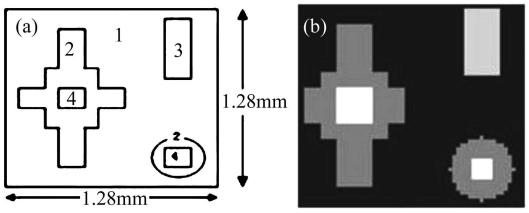

Fig. 2. (a) Shape of the sample used in the simulation. The composition and concentration of the simulation sample is defined in Table 1; (b) Element distribution in the simulation sample.

Table 1. Chemical composition and concentration of the simulation sample.

phase index	concentration (weight %)	
	C, H, O, N ···	Cu
1	100.0	0.0
2	99.0	1.0
3	96.0	4.0
4	94.0	6.0

The fluorescence tomography projections of the test sample were generated algebraically. The simulated scan was performed in 128, 64 and 32 steps with 10μm, 20μm and 40μm sampling intervals for a projection while the angular step was 1, 2 and 5 degree, which yields 180, 90 and 36 projections. In all cases, SR-XFMT images were reconstructed using Hogan's modified FBP algorithm including attenuation correction. The reconstruction SR-XFMT images from simulation data under different sampling interval and a number of projections were shown in Fig. 3(a—i).

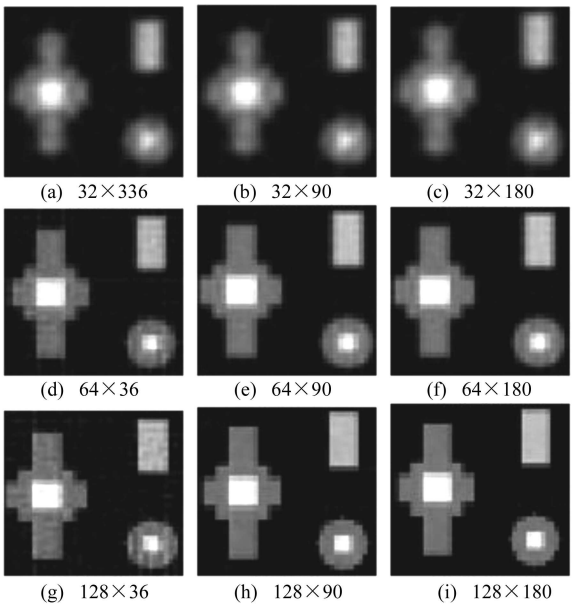

Fig. 3. Reconstructed images from numerical simulation under different sampling interval (number of scan steps(N)) and a number of projections(M).

4 Discussion and conclusion

Usually, the assessment of reconstruction image is based on visual examination and/or computing some mathematical measure(s) of agreement between a reconstructed image and the original object such as the normalized root mean squared distance and the normalized mean absolute distance to quantify the image quality. Three mathematical measures can be taken from the standard measurements used by Herman[17]. The less these measurements are, the better the reconstruction quality becomes. These measurements are defined as follows:

The normalized root mean squared distance measure:

$$d=\left[\frac{\sum_{i=1}^{n\times n}(r_i-p_i)^2}{\sum_{i=1}^{n\times n}(p_i-\bar{p})^2}\right]^{\frac{1}{2}}, \quad (3)$$

The normalized mean absolute distance measure:

$$r=\frac{\sum_{i=1}^{n\times n}|r_i-p_i|}{\sum_{i=1}^{n\times n}|p_i|}, \quad (4)$$

The worst relative error between the phantom and reconstruction:

$$e=\max_{i=1}^{n\times n}\frac{|p_i-r_i|}{p_{\max}-p_{\min}}, \quad (5)$$

where p_i denotes the phantom image value of the ith pixel, r_i denotes the reconstruction image value of the ith pixel, and $\bar{p}$ denotes the average pixel value of p_i. $n\times n$ determines the total quantity of pixels in the image matrix in use. The measurements of reconstruction under different sampling intervals and projections were shown in Table 2.

Table 2. The measurements of the quality of reconstruction under different sampling intervals and projections.

sampling interval	number of scan steps(N)	projections(M)	d	r	e
		180	1.44×10^{-2}	1.50×10^{-2}	1.44×10^{-2}
1	128	90	1.44×10^{-2}	1.52×10^{-2}	7.62×10^{-3}
		36	1.45×10^{-2}	1.62×10^{-2}	4.90×10^{-2}
		180	2.52×10^{-2}	2.32×10^{-2}	2.42×10^{-2}
2	64	90	2.52×10^{-2}	2.32×10^{-2}	3.43×10^{-2}
		36	2.56×10^{-2}	2.48×10^{-2}	6.42×10^{-2}
		180	4.65×10^{-2}	4.04×10^{-2}	5.72×10^{-2}
4	32	90	4.65×10^{-2}	4.04×10^{-2}	5.05×10^{-2}
		36	4.66×10^{-2}	4.10×10^{-2}	0.16

Fig. 3 (a,b,c) are the reconstructed images under different projections with the same 40μm sampling interval. From these images we can see that the quality of image reconstruction does not become better when the number of projections are increased in the same sampling interval. From Table 2 we also can find that the corresponding measurements d, r, e of Fig. 3 (a,b,c) do not become less. From Fig. 3 (d,e,f) , Fig. 3 (g,h,i) and the corresponding measurements in Table 2 we also find that the quality of image reconstruction does not become better when the number of projections are increased in the same sampling interval.

Fig. 3 (c,f,i) are the reconstructed images under different sampling intervals with the same 180 projections. From these images we can see that the boundaries become more and more clear with the sampling interval reducing. From Table 2 we also find that the corresponding measurements do become less with the sampling interval reducing. From Fig. 3 (a,d,g), Fig. 3 (b,e,h) and the corresponding measurements in Table 2 we also find that the quality of image reconstruction does become better when the sampling interval is reduced in the same number of projections.

Fig.3 (c,e) are the reconstruction images of the same ray number ($M\times N$). From the two images we can find that the quality of Fig. 3(e) is better than Fig. 3(c). From Fig. 3(c,e) and the corresponding measurements in Table 2 we find that the quality becomes better when the sampling interval becomes less in the same ray number.

According to Fig. 3, Table 2 and the above discussion, a conclusion on the relationship between the reconstruction quality and the sampling interval and the number of projections can be drawn. It is found that the sampling interval has greater effect on the quality of reconstruction image than the number of the projections. In the real experiment, we can select the suitable sampling interval and the number of projections for reducing cost and improving the quality of image reconstruction in SR-XFMT.

References

1 Boisseau P. Determination of Three-Dimensional Trace Element Distributions by the Use of Monochromatic X-ray Microbeams. Ph.D Dissertation. M.I.T. Cambridge. 1986
2 Hogan J P, Gonsalves R A, Krieger A S. IEEE Trans. Nucl. Sci., 1991, **38**(6): 1721—1727
3 Yuasa T, Akiba M, Takeda T et al. IEEE Trans. Nucl. Sci., 1997, **44**(1): 54—62
4 Rust G F, Weigelt J. IEEE Trans. Nucl. Sci., 1998, **45**(1): 75—88
5 Simionovici A, Chukalina M, Drakopoulos M et al. Proc. SPIE, 1999, **3772**: 304—310
6 Vincze L, Janssens K, Vekemans B et al. Spectrochimica Acta, 1999, **B54**: 1711—1722
7 Vincze L, Janssens K, Vekemans B et al. Proc. SPIE, 1999, **3772**: 328—339
8 Takedaa T, YU Q, Yashiro T et al. Nucl. Instrum. Methods, 2001, **A467–468**: 1318—1321
9 Menez B, Simionovici A, Philippo Pt et al. Nucl. Instrum. Methods, 2001, **B181**: 749—754
10 Schroer C G, Benner B, Gunzler T F et al. Pro. SPIE 2002, **4503**: 230—239
11 Sutton S R, Flynn G J, Rivers M et al. Lunar and Planetary Science, 2000, **31**: 1857—1858
12 Naghedolfeizi M, Chung J S, Ice G E et al., Mat. Res. Soc. Symp. Proc., 1998, **524**: 233—235
13 MENG Y, Newville M, Sutton S et al. American Mineralogist, 2003, **88**: 1555—1559
14 Golosio B, Somogyi A, Simionovici A et al. Apple. Phys. Lett., 2004, **84**(12): 2199—2201
15 Schroer C G. Appl. Phys. Lett., 2001, **79**(12): 1912—1914
16 Golosio B, Simionovici A, Somogyi A et al. J. Appl. Phys., 2003, **94**: 145—156
17 Herman G T. Image Reconstruction from Projections: The Fundamentals of Computerized Tomography. New York: Academic Press, 1980. 66—67

采样间隔和投影数对SR-XFMT重构质量的影响

邓彪　余笑寒[1)]　徐洪杰

(中国科学院上海应用物理研究所　上海　201800)

摘要　同步辐射微束X射线荧光CT(SR-XFMT)是一种能无损、高空间分辨和高灵敏地探测样品内部元素含量和分布的新技术. 对SR-XFMT实验进行了计算机模拟, 讨论了采样间隔和投影数对重构质量的影响, 分析发现采样间隔对重构质量的影响比投影数的影响要大.

关键词　SR-XFMT　图像重构　采样间隔　投影数

2006 – 09 – 12 收稿,　2006 – 11 – 01 收修改稿

1) E-mail: yuxh@sinap.ac.cn